

Co spin fluctuations and long-range ordering in $\text{YBa}_2\text{Cu}_{3-x}\text{Co}_x\text{O}_y$

F. Maury,¹ I. Mirebeau,² V. Viallet,³ and A. Forget⁴

¹Laboratoire des Solides Irradiés, Ecole Polytechnique, 91128 Palaiseau, France

²Laboratoire Léon Brillouin, CEA-CNRS, CE-Saclay, 91191 Gif-sur-Yvette, France

³Laboratoire d'Etudes des Matériaux Hors-Equilibre, Université Paris-Sud, 91405 Orsay, France

⁴Service de Physique de l'Etat Condensé, CEA-CNRS, CE-Saclay, 91191 Gif-sur-Yvette, France

(Received 29 January 2007; revised manuscript received 30 March 2007; published 6 June 2007)

We have studied the magnetic order and spin fluctuations in $\text{YBa}_2\text{Cu}_{3-x}\text{Co}_x\text{O}_y$ ($0.12 < x < 1$) using neutron diffraction, magnetization, and inelastic neutron scattering. In both oxygenated and deoxygenated samples, our results suggest that Co1 moments on chain sites are not collinear but rather perpendicular to Cu2 moments on planar sites, in contrast with what has been previously assumed. The ordered moment on the Co1 ions remains well below the paramagnetic Co moment ($\sim 3\mu_B$), indicating that most of the Co moments remain disordered at low temperature. The study of Co spin fluctuations by inelastic neutron scattering shows the presence of fluctuating spins $d=2a$ pairs that freeze below about 100 K. When the Co concentration increases, they coexist with $d=a$ pairs and other small spin clusters undergoing a gradual freezing. The increasing frustration that arises from the competition of antiferromagnetic first and second neighbor Co pairs is responsible for the low value of the ordered Co moment.

DOI: 10.1103/PhysRevB.75.214410

PACS number(s): 74.72.Bk, 75.40.Gb, 78.70.Nx

I. INTRODUCTION

$\text{YBa}_2\text{Cu}_{3-x}\text{Co}_x\text{O}_y$ compounds offer a good opportunity to study the interplay of magnetism and superconductivity. The Co ions substitute for Cu ones up to $x=1$, mainly on the chain sites.¹⁻³ It was previously shown⁴⁻⁶ that in the oxygenated state ($y \geq 7$) superconductivity (SC) disappears and antiferromagnetic (AF) order settles in for a Co content $x=0.42$. AF order is also stabilized at lower x content in deoxygenated samples.⁷ In this AF state, several magnetic models have been proposed to account for the neutron diffraction patterns. For $y \geq 7$, a simple model where the Co and Cu moments are parallel and align along the c axis yields a good agreement with the experimental data.^{8,9} Surprisingly in this model the Co ordered moment was found to be very small, only about 5% of the value measured in the paramagnetic state. This reduction of the ordered moment was attributed to the competition between AF first and second Co neighbors, yielding a frustration and disorder in the Cu1 (chain) planes.⁹ Still, the previous experiments raised several questions: (1) what occurs when the Cu1 sites are fully substituted by Co? (2) could more complex (uncollinear) magnetic structures also account for the magnetic patterns? (3) could one directly probe the magnetic fluctuations and disorder of the Co moments? To answer these questions, we performed neutron diffraction in a $x=1$ sample, as well as in deoxygenated samples ($x=0.12$ and 0.36). In these new samples, we find that the collinear model previously assumed yields values and temperature dependence of the magnetic moments difficult to understand, and that a noncollinear structure is more likely. We reinvestigate the previous experiments performed at lower x contents⁹ with the assumption of noncollinear structure. We find that a noncollinear structure may also account for these data. In the noncollinear model, the Co ordered moment is substantially higher than in the collinear model, but it remains strongly reduced with respect to the paramagnetic moment measured by magnetization. By probing the spin fluctuations, inelastic neutron scattering al-

lows us to determine the origin of this difference. We evince rapidly fluctuating Co moments in both paramagnetic and ordered phase, and we can follow the slowing down of their fluctuations with decreasing temperature. By analyzing the q dependence of the diffuse scattering we find that the Co moments are highly frustrated. The frustration arises from the competition of antiferromagnetic first and second neighbor Co pairs. By calibrating the quasielastic signal in absolute scale we can show that the proportion of second neighbor pairs decreases as the Co concentration increases, to the benefit of first neighbor and more complex structures, so that there are more and more frustrated pairs. The whole analysis provides a self-consistent picture of the Co magnetism in Co-doped YBCO.

II. EXPERIMENT

Neutron measurements were performed at the Laboratoire Léon Brillouin (LLB). Powder diffraction patterns were recorded on the G61 diffractometer with an incident wavelength of $\lambda=4.741 \text{ \AA}$, in the range $5 < 2\theta < 145^\circ$, i.e., $0.12 < q < 2.5 \text{ \AA}^{-1}$. An additional pattern was recorded on the 3T2 diffractometer ($\lambda=1.225 \text{ \AA}$) in the range $0.8 < q < 9 \text{ \AA}^{-1}$ for the most concentrated sample. The powder patterns were refined using the FULLPROF suite.¹⁰ Inelastic neutron scattering measurements were performed on the time-of-flight spectrometer MIBEMOL of the LLB, with an incident wavelength of 5.2 \AA and an energy resolution [fullwidth at half-maximum (FWHM)] of $70 \mu\text{eV}$. The magnetization measurements were performed with the superconducting quantum interference device (SQUID) of the SPEC Laboratory.

III. SAMPLE CHARACTERIZATION AND CRYSTAL STRUCTURE

The powder samples $\text{YBa}_2\text{Cu}_{3-x}\text{Co}_x\text{O}_y$ ($0.04-0.72$) in their fully oxygenated state ($y \sim 7$) are the same as those

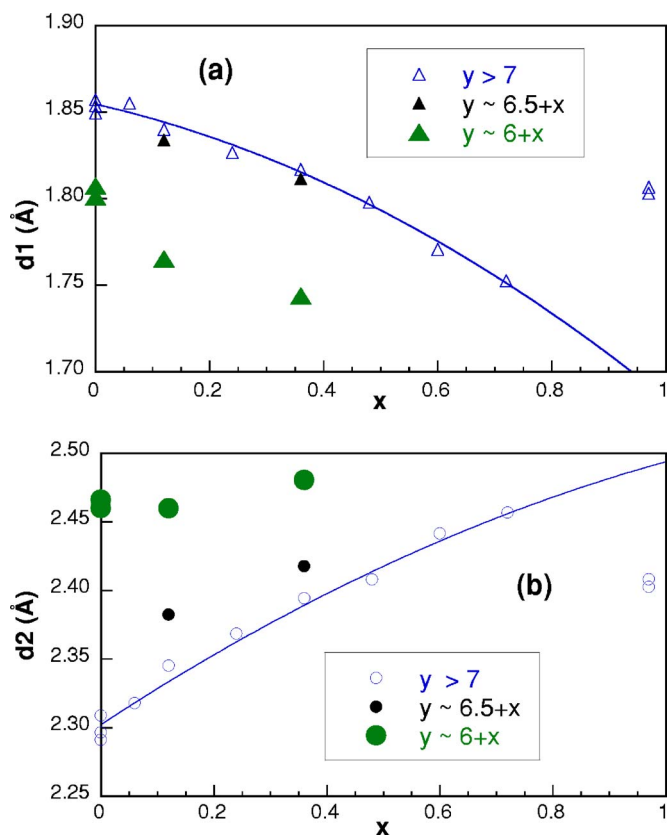


FIG. 1. (Color online) Interatomic distances, (a) $d1 = d(\text{Cu1-O}_{ap})$ and (b) $d2 = d(\text{Cu2-O}_{ap})$ as a function of x , for various Co-YBCO samples: fully oxygenated (open symbols), partially deoxygenated (small full symbols), and totally deoxygenated (large full symbols). The curves are eye-fits to the data.

studied in Ref. 9. These samples are superconducting for $x < 0.42$ and antiferromagnetic for $x > 0.42$. A new sample with $x=1$ was prepared in the same conditions. After being studied, some samples were deoxygenated and remeasured. We prepared two kinds of deoxygenated samples. Three SC oxygenated samples ($x=0.04, 0.12,$ and 0.36) were moderately deoxygenated (at 715 C) to reach an oxygen concentration $y=6.5+x$, which corresponds to a hole concentration in the Cu2 planes between that of $\text{YBa}_2\text{Cu}_3\text{O}_{6.5}$ and 0. The Co ions are $\text{Co}1^{4+}$ (suffixes 1 and 2 refer to chain and plane sites, respectively). Two AF samples were further deoxygenated (at 730 C) to reach a minimal y value. We obtained $y=6.30$ for $x=0.36$ and 6.45 for $x=0.48$. These y values are close to $6+x$, which corresponds to Co ions being on average Co^{3+} . The oxygen concentrations determined by refining the neutron patterns are in good agreement with the measured weight losses. Refinement of the room temperature powder patterns yielded Co occupancies, lattice constants, and positional parameters in agreement with previous results.^{4,6,8,9}

Figure 1 shows the variation of the distances $d1$ and $d2$ between the apical oxygen and the chain and plane sites. In the oxygenated samples, $d1$ decreases with x , as the charge on the Cu1 sites increases (substitution of Co^{4+} ions for Cu^{2+} ones). At the same time $d2$ increases with x , as the charge on the Cu2 sites decreases (suppression of holes in the Cu2 planes). We see that an increase of x has the same effect as

deoxygenation. A moderate deoxygenation has only slight effects on $d1$ and $d2$, whereas a strong deoxygenation decreases $d1$ and increases $d2$, leading to values close to those of $\text{YBa}_2\text{Cu}_3\text{O}_6$. For $x=1$, the data points are not on the curves: in this concentrated sample, 7% of Co ions are in the Cu2 planes (Co^{3+} replacing Cu^{2+}), and part of the Co1 ions are Co^{3+} and not Co^{4+} .

IV. ANTIFERROMAGNETIC ORDER

A. Oxygenated samples

As for of all oxygenated samples with $x > 0.42$, the diffraction patterns of the $x=1$ sample, $\text{YBa}_2\text{Cu}_2\text{Co}_{0.97}\text{O}_{7.25}$, show three magnetic peaks that can be indexed $(1/2 \ 1/2 \ l/2)$ with $l=1, 3, 5$. The $(1/2 \ 1/2 \ 7/2)$ peak, at $2\theta=112^\circ$, between the $(0 \ 0 \ 4)$ and $(0 \ 1 \ 3)$ nuclear peaks, does not clearly show up above the background. We deduced the mean ordered magnetic moments on the Cu1 and Cu2 sites by assuming as in Ref. 8 and in our previous work,⁹ that the Co1 and Cu2 spins are collinear. Again, we could not fit the data with spins parallel to an in-plane direction but we obtained a good fit with spins perpendicular to the Cu2 planes. The refined values of the low temperature ordered magnetic moments on the Cu1 and Cu2 sites are $\mu_0(\text{Cu1})=0 \pm 0.02\mu_B$ and $\mu_0(\text{Cu2})=0.80 \pm 0.02\mu_B$. Contrary to what we expected, $\mu_0(\text{Cu1})$ is not increased as compared to the lower Co concentrations but decreased down to about 0. Moreover, $\mu_0(\text{Cu2})$ is larger than expected for a Cu2 plane with no hole, namely $0.63\mu_B$ with an isotropic Cu form factor.¹¹ It is unlikely that this increment is due to the Co^{3+} ions in the Cu2 planes since these ions should be low spin and carry no magnetic moment. Added to that, it is difficult to understand why, at lower concentrations with no Co in the Cu2 planes, the Cu2 ordered moment is still larger than that expected (see Fig. 7 of Ref. 9) and how the weak Cu1-Cu2 interaction can turn the Cu2 moments along the c axis. We notice that using an anisotropic form factor, as justified from Refs. 12 and 13 would reduce all magnetic moments in the same way, without changing these conclusions.

We thus tried to refine the diffraction patterns by assuming that the Co1 and Cu2 moments are not collinear but that the Cu2 moments lie along the a axis, as in YBCO6, and the Co1 moments have two components, one parallel to \mathbf{c} and one, μ_a , parallel to \mathbf{a} , i.e. to the Cu2 moments. Actually our powder diffraction measurements cannot determine any preferential direction in the (a, b) plane, but the existence of a small in-plane anisotropy is shown in AF YBCO by neutron measurements in single crystals.¹⁴ The fit quality is the same for the two models (typically $R_B=3\%$, $R_M=6\%$). The refined value of $\mu(\text{Cu1})$ and $\mu(\text{Cu2})$ in the noncollinear model are shown as a function of the temperature in Fig. 2(a). The value of $\mu_0(\text{Cu2})$ is now as expected ($0.60 \pm 0.07\mu_B$) and $\mu_0(\text{Cu1})$ is no longer zero ($0.70 \pm 0.05\mu_B$). The component μ_a of the Co1 moments is small; the Co1 moments are thus lying near the \mathbf{c} axis as in the collinear model. The Co1/Cu1 moments are AF coupled with their Cu2/Co2 nearest neighbors.

We also refined with this model the diffraction patterns measured in Ref. 9. Again the fit quality is similar for both

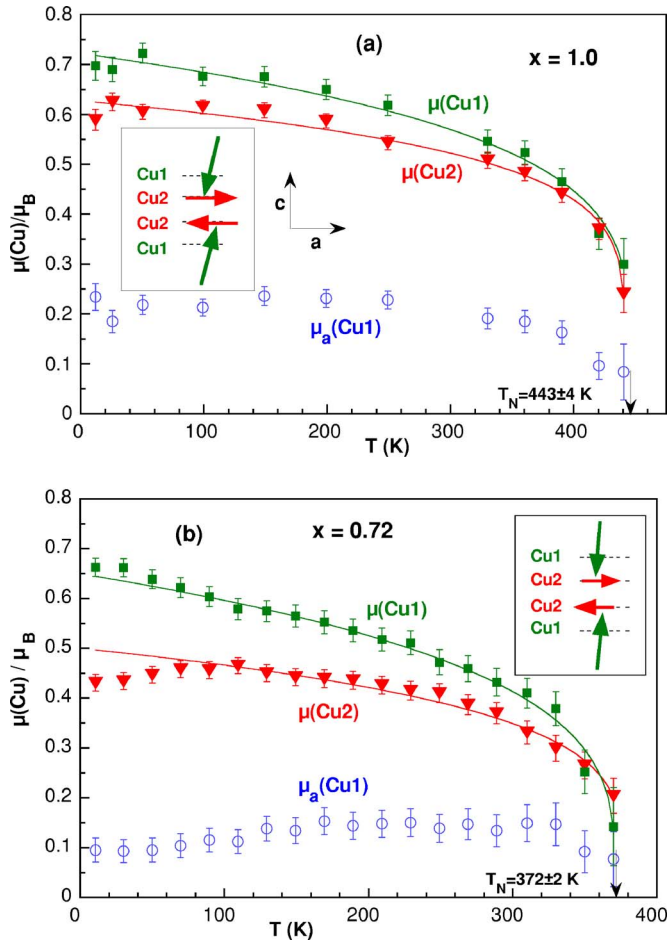


FIG. 2. (Color online) Long-range ordered magnetic moments on the Cu1 sites (squares) and on the Cu2 sites (triangles) for fully oxygenated $\text{YBa}_2\text{Cu}_{3-x}\text{Co}_x\text{O}_y$ samples with (a) $x=1.0$ and (b) $x=0.72$. These values were refined with $\mu(\text{Cu2})$ parallel to \mathbf{a} and $\mu(\text{Cu1})$ near the \mathbf{c} axis with a small component parallel to \mathbf{a} (circles). The curves are fits with the formula $\mu = \mu_0 (1 - T/T_N)^\beta$. For $\mu(\text{Cu2})$, β does not depend much on x , $\beta = 0.18 \pm 0.03$. For $\mu(\text{Cu1})$, β decreases from 0.45 to 0.2 as x increases from 0.6 to 1.

models (typically $R_B=1\%$, $R_M=5\%$). The results are shown in Fig. 2(b) for $x=0.72$. Figure 3 shows the low temperature ordered magnetic moments on the Cu1 and Cu2 sites as a function of x . We see that in the noncollinear model [Fig. 3(b)], the collinear component of the Cu1 and Cu2 moments, $\mu_a(\text{Cu1})$, increases linearly with x . At low x content, the Cu1 and Cu2 moments are practically perpendicular. Yet, $\mu_a(\text{Cu1})$ cannot be null to ensure the coupling between the Cu1 and Cu2 planes.

One gets similar results by assuming that the Cu1 moments lie along the \mathbf{c} axis and the Cu2 moments have two components, one parallel to \mathbf{a} and one parallel to \mathbf{c} , i.e., parallel to the Cu1 moments. The Cu2 moments are found roughly parallel to \mathbf{a} and their magnitude as well as that of the Cu1/Cu1 ones are very near those found before. The difference is within the uncertainty limits.

Thus we can conclude that the noncollinear model yields Cu1 moments roughly parallel to \mathbf{c} and Cu2 moments roughly parallel to \mathbf{a} , those moments having a small collinear

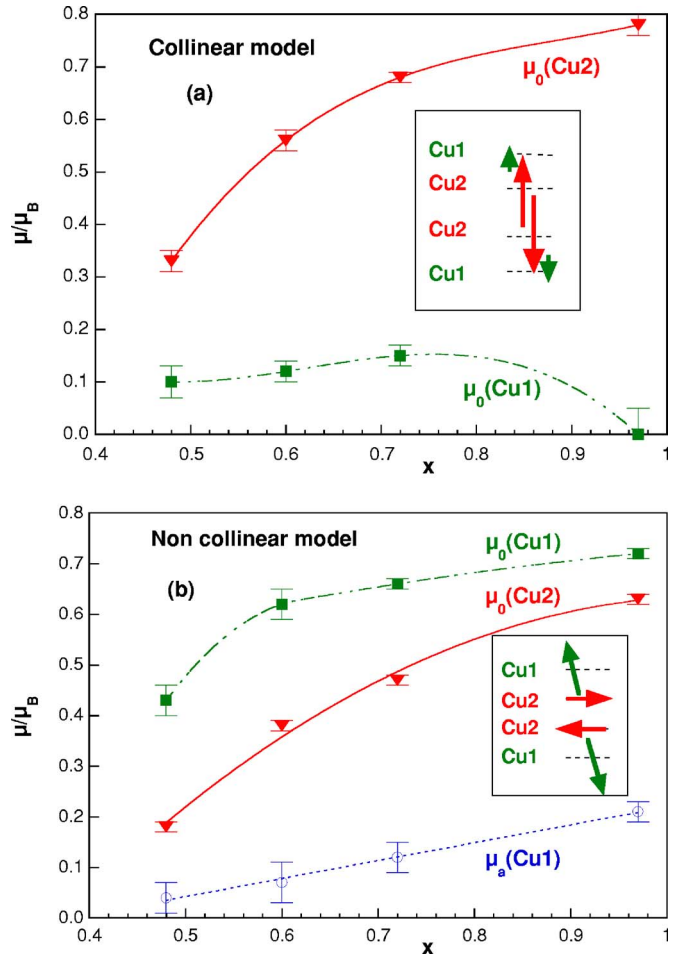


FIG. 3. (Color online) Low temperature LR ordered magnetic moments on the Cu1 and Cu2 sites as a function of x (same symbols as in Fig. 2).

component whose direction cannot be ascertained. Compared to the collinear model, the noncollinear model yields larger values for $\mu_0(\text{Cu1})$. These values are even larger than $\mu(\text{Cu2})$. Yet they remain significantly smaller than the paramagnetic value that is deduced from magnetization measurements (see Sec. V).

B. Moderately deoxygenated samples

The $x=0.04$ sample is SC, $x=0.12$ is AF up to 240 K and $x=0.36$ AF up to 400 K. The AF samples exhibit two different long-range (LR) magnetic order according to the temperature. At low temperature, the observed $(1/2\ 1/2\ l/2)$ magnetic peaks are those with $l=1, 3, 5$, as in Co-YBCO7. At higher temperature, this structure transforms to the structure observed in YBCO6, with $(1/2\ 1/2\ l)$ magnetic peaks where $l=1, 2$. In a limited domain of intermediate temperatures, the two series of magnetic peaks are observed simultaneously (see Fig. 4). The coexistence region is small: a few degrees around $T=30$ K for $x=0.12$ and from 80 to 110 K for $x=0.36$.

At high temperature, the magnetic moments on the Cu1 sites are null and the diffraction patterns are best fitted with

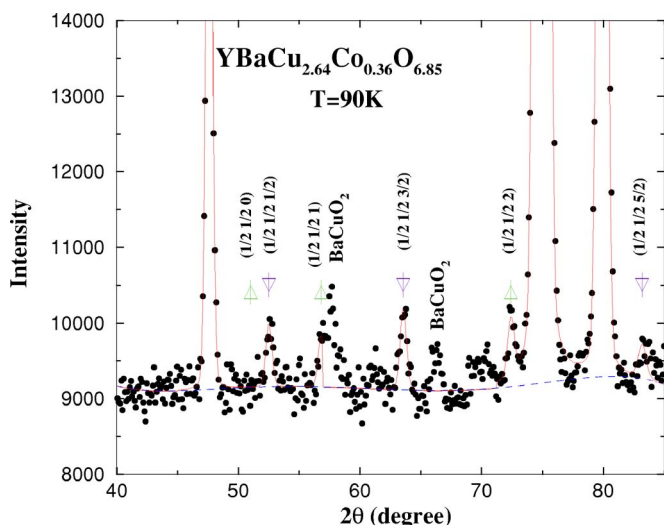


FIG. 4. (Color online) Diffraction pattern for $x=0.36$, $y=6.85$ ($p \sim 0$), at a temperature $T=90$ K where the two structures AF2 and AF1 coexist. Two series of peaks, $(1/2 \ 1/2 \ l/2)$ with $l=1, 3, 5$ and $(1/2 \ 1/2 \ l)$ with $l=1, 2$, are observed. The solid line is the FULL-PROF refinement of the data with the non collinear model. The dashed line is a polynomial background.

Cu2 spins parallel to the a axis as in YBCO6. Now the low temperature patterns were first refined with a collinear model. As for the Co-YBCO7 samples, no good fit could be obtained with in-plane moments but a good fit was obtained with Cu1 and Cu2 moments both parallel to c . The ordered magnetic moments are shown as a function of the temperature in Fig. 5(a). We see that in the intermediate region, $\mu(\text{Cu2})$ exhibits an important change of magnitude that is not readily understandable.

We then refined the low temperature patterns with a non-collinear model. As for the oxygenated $x=0.48$ sample, the moments on the Cu1 and Cu2 sites are found almost perpendicular: the collinear component, $\mu_a(\text{Cu1})$, is smaller than the uncertainty on its determination ($0.05\mu_B$). The refined values of the ordered magnetic moments on the Cu1 and Cu2 sites are shown on Fig. 5(b). We see that the orientation as well as the magnitude of the magnetic moments on the Cu2 sites are similar in the low and high temperature phases: $\mu(\text{Cu2})=0.3\mu_B$ for $x=0.36$ and $0.25\mu_B$ for $x=0.12$.

Assuming that in the intermediate region, the two periodicities coexist due to slightly different local oxygen concentrations or Co1 distributions, we have calculated the ordered magnetic moment on the Cu2 sites in this region (diamonds in Fig. 5). We see that $\mu(\text{Cu2})$ does not evince any discontinuity with the noncollinear model while it displays an important change with the collinear model. Again, the noncollinear model seems more likely than the collinear one.

C. Fully deoxygenated samples

The two ($x=0.36$, $y=6.30$) and ($x=0.48$, $y=6.45$) samples have the same transition temperature as YBCO6 ($T_N=420$ K), but their magnetic structure is different. The magnetic patterns show $(1/2 \ 1/2 \ l/2)$ magnetic peaks with $l=1,$

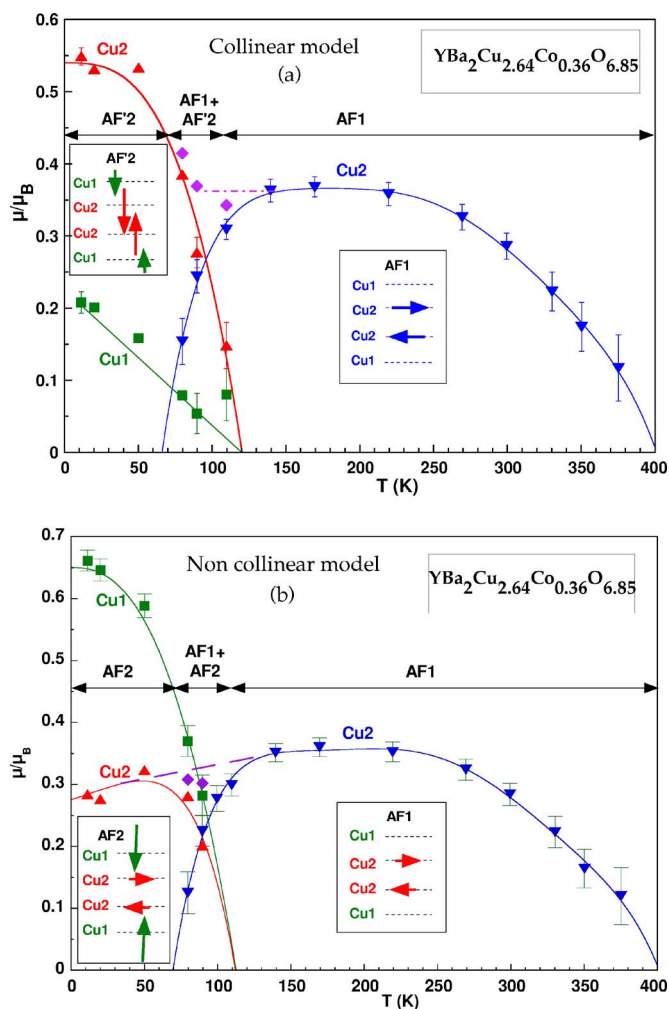


FIG. 5. (Color online) LR ordered moments on the Cu1 (squares) and Cu2 sites (triangles) for the ($x=0.36$, $y=6.85$) sample. (a) $\mu(\text{Cu1})$ and $\mu(\text{Cu2})$ in the AF'2 phase are collinear and parallel to c ; $\mu(\text{Cu2})$ in the AF1 phase is parallel to a (b) $\mu(\text{Cu2})$ is parallel to a and $\mu(\text{Cu1})$ in the AF2 phase is parallel to c . In the intermediate region, $\mu(\text{Cu2})$ (diamonds) is deduced by assuming the coexistence of two kinds of domains, with AF1 or AF2 structure.

3, 5, as in Co-YBCO7. Yet the $l=1/2$ magnetic peak, instead of being the most important of the first three peaks, is now the smallest. For these two samples, the collinear model yields Co1 and Cu2 moments parallel to a and not parallel to c . $\mu(\text{Cu1})$ is weak (below $0.05\mu_B$) and $\mu(\text{Cu2})$ around $0.6\mu_B$, as expected for Cu2 planes with no holes.

With the noncollinear model, $\mu(\text{Cu2})$ stays close to $0.6\mu_B$. The collinear component of the Co1/Cu1 moments $\mu_a(\text{Cu1})$ stays weak, slightly outside the uncertainty limit. But now, the component of $\mu(\text{Cu1})$ along the c axis is not negligible, around $0.2\mu_B$: as in the more oxygenated samples, the Co moments are roughly parallel to c but, now they are smaller than the Cu2 moments, which can be explained by part of the Co1 ions being Co^{3+} with no magnetic moment. Finally, for those samples, both models yield equally acceptable results.

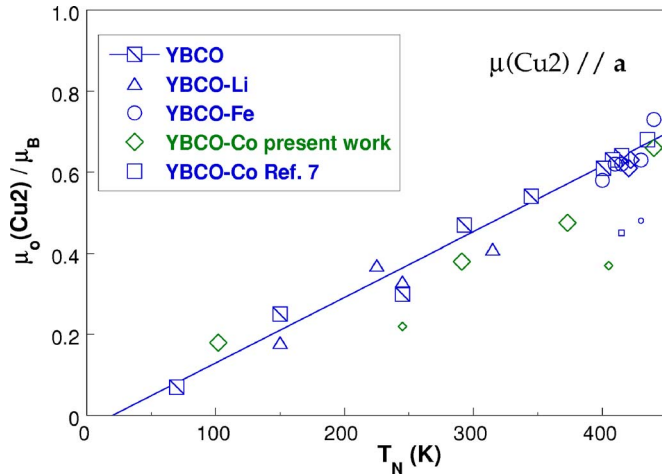


FIG. 6. (Color online) LR ordered magnetic moment on the Cu2 sites measured at 10 K in various YBCO samples, as a function of T_N . The large symbols correspond to samples where only one structure, AF1 or AF2, is observed, the small symbols correspond to samples where AF1 and AF2 structures are successively observed.

D. Summary of diffraction results

The whole set of our data are best explained by (i) ordered Cu2 moments always lying in (as in other CuO2 systems) or near the Cu2 planes, and ordered Co1 moments close to the c axis. (ii) The collinear component of the Cu1 and Cu2 moments is small. The Cu1 and Cu2 planes are weakly coupled. (iii) $\mu(\text{Cu2})$ depends on the hole concentration in the Cu2 planes and not much on the Co concentration. By decreasing the hole concentration in the Cu2 planes, the Co1 substitution like deoxygenation increases $\mu(\text{Cu2})$, from 0 for fully oxygenated samples with low Co concentrations, to about $0.25\mu_B$ for moderately deoxygenated samples of medium Co concentration, and up to about $0.6\mu_B$ (as for YBCO6) for fully deoxygenated samples or high Co concentrations.

As already known, the Cu2 moments are long-range (LR) ordered up to a temperature T_N that depends on the coupling in the Cu2 planes much more than on the coupling between the biplanes. If we compare the fully deoxygenated samples, we see that $T_N \sim 420$ K for $x=0$, $x=0.36$, and $x=0.48$. The Co ions only influence the stacking of the Cu2 biplanes: ferromagnetic stacking (AF1) for $x=0$ and antiferromagnetic stacking (AF2) for $x=0.36$ and $x=0.48$.

Figure 6 displays $\mu_0(\text{Cu2})$ as a function of T_N for different M -YBCOy systems where M is a substitute for Cu, either on the Cu1 or on the Cu2 sites. We see that, with the present model (Cu2 spins in Cu2 planes), contrary to the collinear model (Cu2 spins perpendicular to Cu2 planes), $\mu_0(\text{Cu2})$ scales with T_N with the same scaling constant for all single phase systems, whether the structure is AF1 (YBCO6 and Li-YBCO6) or AF2 (Fe-YBCO and Co-YBCO). This scaling does not hold when two different magnetic phases are observed depending on the temperature. We can imagine that due to the competition between the two structures, AF1 and AF2, stacking faults occur along the c axis, depending on local conditions, and reduce the LR ordered magnetic moments on the Cu1 and Cu2 sites.

Contrary to $\mu_0(\text{Cu2})$ which is increased, $\mu_0(\text{Cu1})$ is decreased by a total deoxygenation: from 0.65 to $0.22\mu_B$ for $x=0.36$ and from 0.4 to $0.2\mu_B$ for $x=0.48$. Two reasons can explain this reduction: (i) less Co ions carry a magnetic moment, due to the transformation of part of the Co^{4+} into non-magnetic Co^{3+} and (ii) the remaining Co^{4+} spins experience a weaker coupling, either because they are fewer and farther from one another, or because the removal of the chain oxygens hinders the exchange. To check the first point, we determined the mean paramagnetic moment of the Co ions in these samples.

V. MAGNETIZATION RESULTS

We measured with a SQUID magnetometer the magnetic susceptibility, from room temperature down to 10 K, for the samples listed in Table I. Figure 7 displays the obtained results for $x=0.36$, with different oxygen concentrations [Fig. 7(a)], and for $x=0.48$ and 0.72 [Fig. 7(b)]. The data have been fitted with a Curie-Weiss law according to the formula $\chi = \chi_0 + C/(T + \theta)$. Such a fit is not expected to work when the samples become either SC or AF. The fitting range was thus limited to $(T_{\min}, 300$ K).

For all samples but one ($x=0.72$), the values obtained for C and θ do not depend much on T_{\min} provided the lowest temperatures are excluded. To get rid of the low temperature effects when comparing the different samples, a constant value of $T_{\min}=90$ K was chosen. The mean paramagnetic moment μ_{para} can be deduced from the C value, according to the formula $C = N\mu_{\text{para}}^2$, which assumes a number N of magnetic moments of equal value. The obtained values of μ_{para} and θ are given in Table I. Column 1 shows μ_{para} per Cu1 site, assuming that the Cu2 moments are not seen. They are indeed not seen in YBCO7, due to the AF correlations in the Cu2 planes. And we have seen that the presence of cobalt in the Cu1 planes has but a small effect on the Cu2 planes. Column 2 shows μ_{para} per Co1 ion, assuming that the Cu1 ions are not seen for similar reasons. For comparison, column 3 shows the ordered magnetic moment per Co1 ion at $T=0$, $\mu_0(\text{Co1})$, measured by neutron diffraction.

A. Oxygenated samples

For all oxygenated samples, we find a roughly constant value $\mu_{\text{para}}/\text{Co1}$ of $(3.3 \pm 0.2)\mu_B$. On the contrary, the Curie-Weiss temperature θ increases regularly with the Co concentration. This increase can be attributed to the increase of the AF interactions between the Co1 moments when the Co concentration increases. If we look at the two samples that are AF ordered at low temperature ($x=0.48$ and 0.72), we see that $\mu_{\text{para}}/\text{Co1}$ (column 2) is much larger than $\mu_0(\text{Co1})$ (column 3): only a few percents of the paramagnetic moments (3% and 5%, respectively) are LR ordered at low temperature.

B. Moderately deoxygenated samples

In the ($x=0.36$, $y=6.85$) sample, $\mu_{\text{para}}/\text{Co1}$ is about $3.0\mu_B$, near its value in the oxygenated $x=0.36$ sample. Deoxygenation does not change the Co moments but en-

TABLE I. T_c is the onset temperature of the SC transition and T_{N1} the transition temperature below which the Cu1 moments are LR ordered. $T_{N1}=T_N$ except for $x=0.36$, $y=6.85$ where $T_N=400$ K. μ_{para} and θ are deduced from a Curie-Weiss fit of the data, $\chi=\chi_0+C/(T+\theta)$, between 90 K and room temperature. The uncertainty on $\mu_{\text{para}}/\text{Co1}$ is $\pm 0.2\mu_B$, that on θ is of a few K. $\mu_0/\text{Co1}$ was deduced with the noncollinear model under the two extreme hypotheses: the ordered moment on the Cu1 ions is zero (upper limit of $\mu_0/\text{Co1}$) or equal to $\mu_0(\text{Cu2})$ (lower limit).

x	y	SC/AF	T_c (K)	T_{N1} (K)	1 $\mu_{\text{para}}/\text{Cu1}$ (μ_B)	2 $\mu_{\text{para}}/\text{Co1}$ (μ_B)	3 $\mu_0/\text{Co1}$ (μ_B)	4 θ (K)
0.04	7.00	SC	92 ^a		<0.8 ^b	<4.0 ^b		10
0.36	7.03	SC	22		1.9	3.2		23
0.42	7.03				2.1	3.2		34
0.48	7.05	AF		100	2.35	3.4	0–0.6	45
0.72	7.10	AF		370	2.75	3.3	0.7–0.8	70
0.36	6.85	AF		110	1.8	3.0	1.0–1.1	44
0.36	6.30	AF		420	1.55	2.6	0–0.4	32
0.48	6.45	AF		420	1.8	2.6	0–0.3	36

^aFor this sample, SC below 92 K, $T_{\text{min}}=105$ K.

^bOnly an upper limit of μ can be determined since at such a low Co content, a possible contribution of BaCuO₂ may not be negligible.

hances the AF interaction between these moments, as shown by the increase of the Curie-Weiss temperature (44 K instead of 23 K), and the onset of AF order at low temperature.

This sample, like the ($x=0.48$, $y=7.05$) one, shows a AF1 to AF2 transition around 100 K, which means that Co spins get LR ordered below 100 K. One effectively observes for these two samples, a slight departure from a Curie-Weiss law below about 90 K [see Figs. 7(a) and 7(b)], consistent with the ordering of only a small part of the paramagnetic Co moments (13% for $x=0.36$).

C. Fully deoxygenated samples

These two samples ($x=0.36$, $y=6.51$) and ($x=0.48$, $y=6.3$) are AF up to 420 K. Figure 7 shows that even in the LR ordered AF phase, the Curie-Weiss law is well obeyed. This is consistent with the fact that only a small part of the Co moments is ordered. The comparison of $\mu_0(\text{Co1})$ and $\mu_{\text{para}}/\text{Co1}$ yields an upper limit of 2% and 1%, respectively, for the fraction of LR ordered moments.

Such a small fraction of ordered moments cannot explain that $\mu_{\text{para}}/\text{Co1}$ ($2.6\mu_B$) is less than before deoxygenation ($3.2\mu_B$). We must then assume that a fraction of the Co ions have reduced their oxidation state and consequently their magnetic moment. This fraction is not negligible: in a simple model where, before deoxygenation, all Co ions have a paramagnetic moment of $3.2\mu_B$ and, after deoxygenation, have either a $3.2\mu_B$ or a null moment, about $\frac{1}{3}$ of the Co ions have lost their moment.

This is not sufficient to explain the strong decrease of $\mu_0(\text{Cu1})$ with deoxygenation, which is by a factor of 3 (from 0.65 to $0.2\mu_B$): not only the number of magnetic Co ions is reduced, but also the AF interaction between them, which is consistent with the decrease of θ .

D. Summary of SQUID results

Even taking into account the uncertainty of the paramagnetic moment determination, we always find that the para-

magnetic moment $\mu_{\text{para}}/\text{Co1}=3.3(2)\mu_B$ is much larger than the LR ordered moment at low temperature deduced from neutron diffraction [$\mu_0(\text{Co1})\leq 1.1\mu_B$]. We thus face the question: why do the Co1 spins, contrary to the Cu2 ones, not order at low temperature? We have suggested⁹ that the long-range ordering of the Co spins is hindered by the competition between an AF interaction between first and second nearest neighbors. In the next section, we directly probe by inelastic neutron scattering (INS) the spin fluctuations of the frustrated paramagnetic Co moments and their random freezing.

VI. INELASTIC NEUTRON SCATTERING RESULTS

We studied, between 30 and 175 K, three oxygenated samples: one ($x=0.72$) LR AF ordered up to 370 K, i.e., in the whole temperature range investigated here, one ($x=0.48$) LR AF ordered up to 100 K and one ($x=0.42$) that does not show any LR ordering. In these three samples we observed a quasielastic signal that is not observed^{15,16} in unsubstituted YBCO7, where the Cu spin fluctuations occur in a higher energy range.¹⁷ The experiment does not evidence much difference, as concerns the quasielastic signal, between the various samples, either AF ($x=0.72$), or not ($x=0.42$) or even SC ($x=0.18$ of Ref. 18). Not much difference is observed either between 75 K and 125 K for the $x=0.48$ sample that is LR ordered at low temperature with a transition temperature $T_N=100$ K.

A. Quasielastic intensity as a function of temperature

We assumed the quasielastic signal to be Lorentzian and we fitted the data using the analytic form

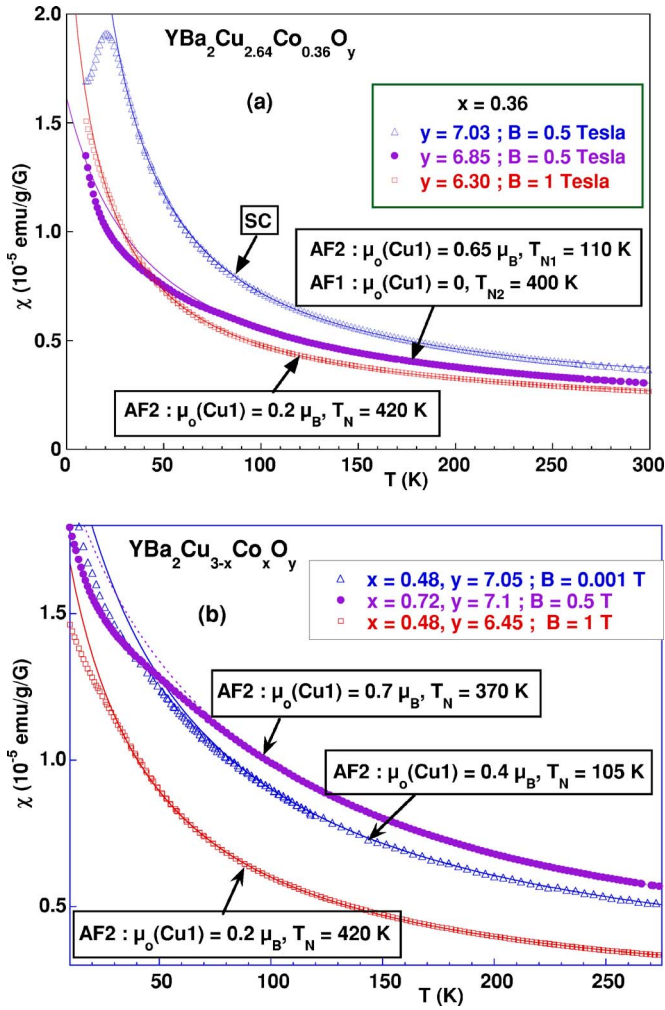


FIG. 7. (Color online) (a) ZFC magnetic susceptibility measured as a function of temperature for $x=0.36$, oxygenated (open triangles), moderately deoxygenated (solid circles), and fully deoxygenated (open squares). (b) Same as (a) for oxygenated $x=0.48$ (open triangles) and $x=0.72$ (solid circles) and for fully deoxygenated $x=0.48$ (open squares) samples. The lines are Curie-Weiss fits to the data for $T \geq 90$ K.

$$\frac{d^2\sigma}{d\Omega d\omega} = C_1\delta(\omega) + \frac{C_2 k_f \omega}{\pi k_i kT} \frac{1}{(\exp^{\omega/kT} - 1)} \frac{\Gamma}{\Gamma^2 + \omega^2} + C_0, \quad (1)$$

convoluted with the experimental resolution. In this equation, ω is the energy gain of the neutron, k_f and k_i are the final and incident wave vectors, C_1 is the elastic intensity, C_2 and Γ are the quasielastic intensity and linewidth, respectively, C_0 is a background including a Debye phonon term and a linear term. Figure 8 shows an example of such a fit, with the different components of the intensity.

Figure 9 shows the elastic and quasielastic intensities as a function of the temperature for the two samples $x=0.42$ and $x=0.72$. The data have been gathered in the range $1.1 < q < 1.6 \text{ \AA}^{-1}$ (that is $55 < 2\theta < 81^\circ$), the magnetic Bragg peaks $(1/2 \ 1/2 \ 1/2)$ and $(1/2 \ 1/2 \ 3/2)$ being excluded when present. In the three investigated samples, $x=0.42, 0.48,$ and

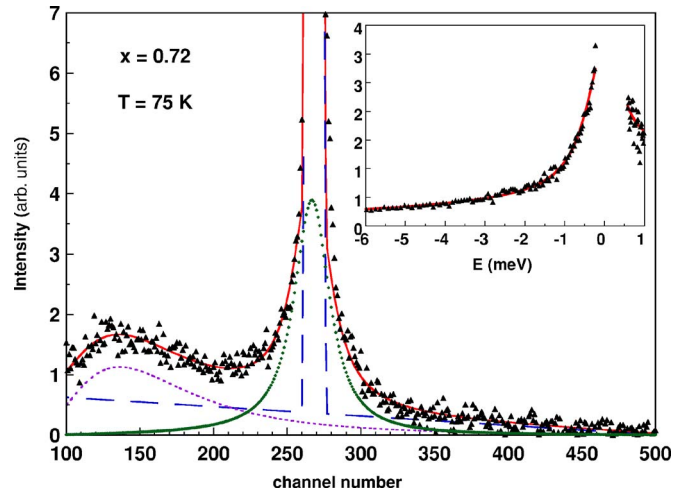


FIG. 8. (Color online) Time-of-flight spectrum for $x=0.72$ at 75 K. The triangles are the experimental data. The curves are the various components of the intensity as determined by the fitting program. The dotted line, dashed line, diamonds, and solid line correspond, respectively, to the phonon background, elastic intensity plus linear background, quasielastic intensity, and total calculated intensity. Inset, the corresponding neutron cross section versus energy transfer. Solid line, fit to the data.

0.72 , the quasielastic integrated intensity (C_2) decreases when the temperature goes down below 75 K. This decrease, associated with an increase of the elastic intensity $C_1(T)$ and with a decrease of the quasielastic width $\Gamma(T)$, suggests that

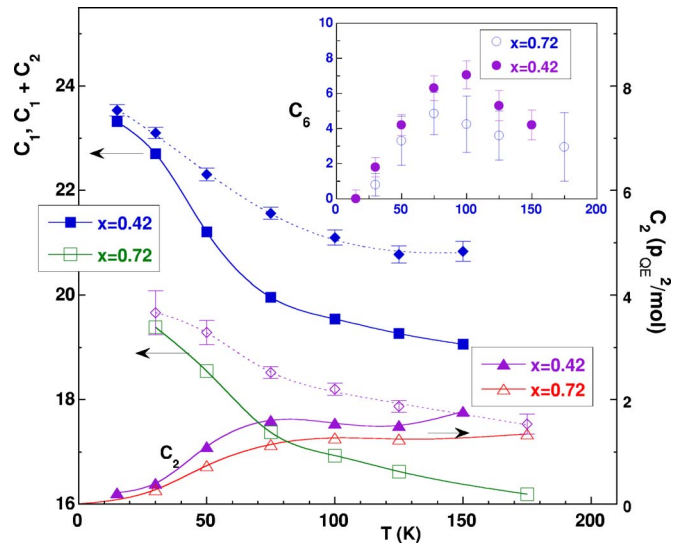


FIG. 9. (Color online) Elastic (squares) and quasielastic (triangles) intensities summed in the interval $1.1 < q < 1.6 \text{ \AA}^{-1}$ for the two oxygenated $x=0.42$ (full figures) and $x=0.72$ (open figures) Co-YBCO samples. The units are the same for C_1 and C_2 , chosen so that the C_2 values are equal to $\mu_{QE}^2/\mu_B^2/\text{mol}$, where μ_{QE} is the mean magnetic moment of the fluctuating spins. The inset shows the linear background level (not including the phonons) as a function of the temperature. The diamonds correspond to the sum of the elastic and quasielastic intensities.

some spin fluctuations, slowing down as the temperature decreases, become too slow to contribute any longer to the quasielastic signal.

B. Elastic intensity as a function of temperature

The decrease of the inelastic intensity due to spin freezing below 75 K, ΔC_2 , must give rise to a concomitant increase of the elastic intensity (C_1). We do observe an increase of C_1 , ΔC_1 , when T goes down below 75 K but this increase is almost 3 times larger than the decrease of C_2 . We are thus led to assume that the decrease of the quasielastic signal ΔC_2 is partially masked by the entrance in this signal of more rapidly fluctuating spins that were not seen at higher temperature and become visible only because their fluctuations are slowed down as the temperature goes down. This interpretation is corroborated by the existence of a flat background (or very broad peak) whose intensity decreases as the temperature goes down from 75 to 15 K (see inset in Fig. 9; C_6 measures the height of the linear background at the upper limit of the time-of-flight interval).

C. Quasielastic intensity as a function of the wave vector

Figure 10(a) shows that the quasielastic intensity observed at $T=75$ K for the $x=0.42$ sample. The data were gathered within eight q ranges, between the Bragg peaks in order to avoid the overwhelming contribution of those peaks, and also, for the $x=0.72$ sample, in the q range of the $(1/2\ 1/2\ 1/2)$ and $(1/2\ 1/2\ 3/2)$ magnetic peaks. We see that C_2 is not a regularly decreasing function of q as expected for uncorrelated spins but oscillates in the investigated q range. The oscillation is well pronounced for $x=0.42$ and $x=0.48$. It is attenuated for $x=0.72$ [Figs. 10(b) and 10(c)]. A fitting of the data assuming randomly distributed AF correlated moments as in Ref. 9 for the diffuse magnetic signal of the diffraction experiment, shows that at low concentration ($x=0.42$ and 0.48), this oscillation can entirely be attributed to pairs of AF coupled spins, separated by a distance d of about 8 Å. If we assume a possible contribution of uncorrelated moments or of AF pairs distant of $d=a$ (as in the LR AF order observed at low temperature), this contribution is given as slightly negative by the fitting program, in the limit of the uncertainty, showing that it is indeed negligible. The refined value of the distance d is 8.3 ± 0.3 Å for $x=0.42$, $T=75$ K, 8.0 ± 0.3 Å for $x=0.48$, $T=75$ K, and 8.2 ± 0.5 for $x=0.48$, $T=125$ K. These d values, smaller than the distance between two Cu1 planes ($c=11.7$ Å) stand between the two following interatomic distances: $2a=7.77$ Å and $a\sqrt{5}=8.68$ Å, in the Cu1 planes. At higher concentration [$x=0.72$, Figs. 10(b) and 10(c)], the oscillation is not as clearly visible as at low concentration. This lessening is attributable to the presence of a small fraction of fluctuating AF correlated pairs distant of a , also evinced by the diffraction experiment.⁹ A contribution of uncorrelated frustrated moments is also possible. Meanwhile, the distance d decreases: $d=7.55\pm 0.25$ Å for $x=0.72$, $T=75$ K. These AF pairs, in their fluctuating as well as frozen state, give rise to a strong magnetic diffuse diffraction peak.⁹ The diffraction

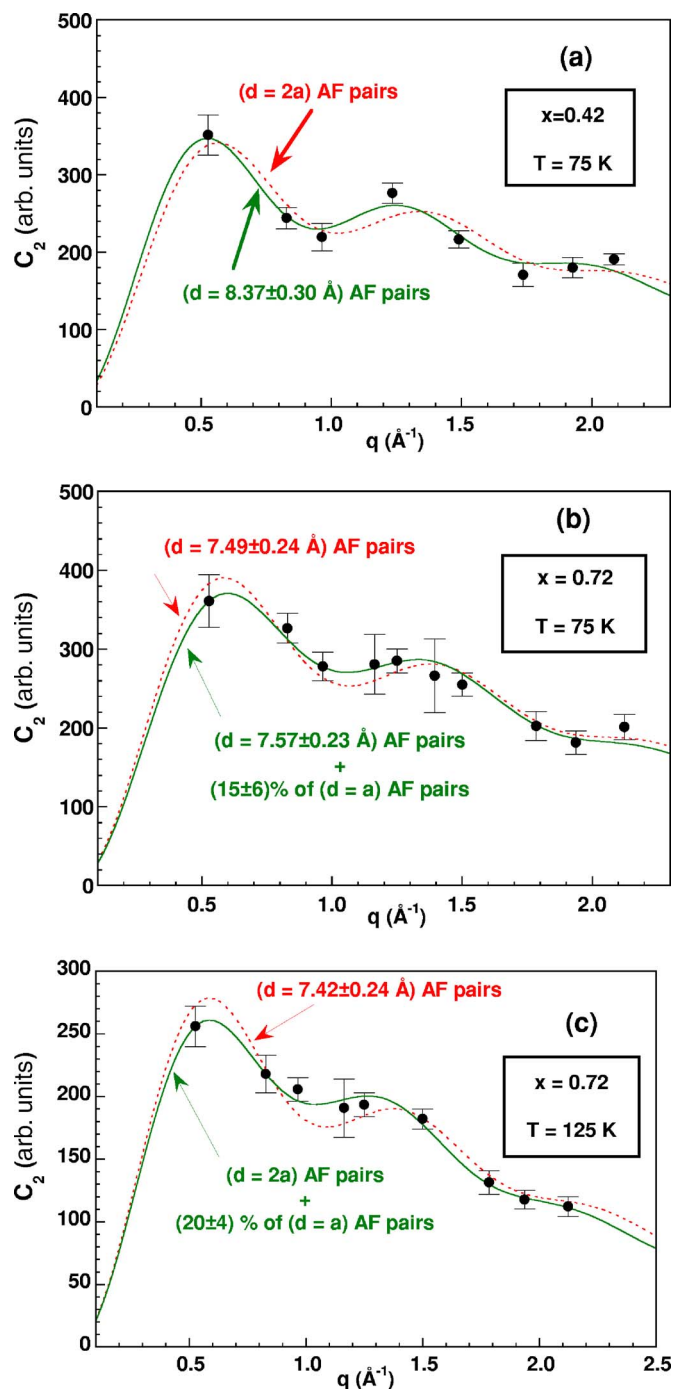


FIG. 10. (Color online) Quasielastic intensity as a function of q . (a) $x=0.42$, $T=75$ K; (b) $x=0.72$, $T=75$ K; (c) $x=0.72$, $T=125$ K. Lines are fits with the formula $C_2 = \exp(-bq^2) \{B_0 + B_1[1 - \sin(qa/2)/(qa/2)] + B_2[1 - \sin(qd/2)/(qd/2)]\}$ with five independent parameters b , B_0 , B_1 , B_2 , and d . B_0 , B_1 , and B_2 correspond, respectively, to uncorrelated spins, correlated spin pairs distant by a (3.885 Å), and correlated spin pairs distant by d .

pattern analysis shows like the INS results, that the distance d decreases with concentration, from $d=8.06\pm 0.06$ Å for $x=0.36$ to $d=7.7\pm 0.1$ Å for $x=0.72$.

We attribute the quasielastic signal to Co-Co pairs for the following reasons: (i) the Cu-Cu spin fluctuations are too rapid and of too small intensity to be probed in unsubstituted

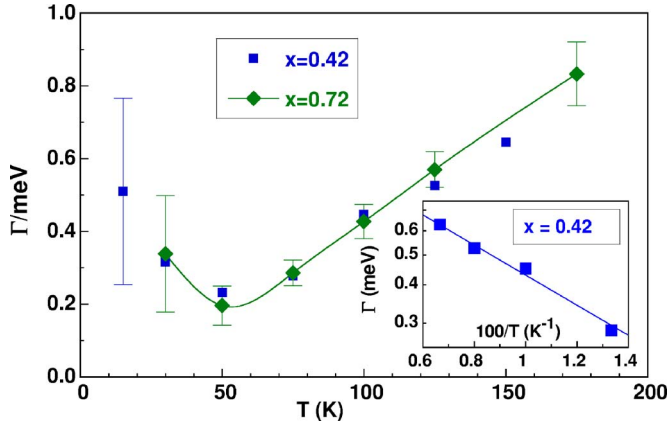


FIG. 11. (Color online) Quasielastic peak width Γ (HWHM) as a function of the temperature, for the three samples $x=0.42$, 0.48 , and 0.72 . The line is an eye-fit to the data. Inset, $\Gamma=f(1/T)$ for $x=0.42$ and $T>50$ K. The line is an Arrhenius fit to the data, $\Gamma=A \exp(-E/kT)$, with $A=1.3$ (1) meV and $E=10$ (1) meV.

YBCO under these experimental conditions;^{15,16} (ii) the amplitude of the signal increases when the Co concentration increases from $x=0$ to about 0.4 ; (iii) the decrease of the distance d with increasing Co concentration is readily understandable if the corresponding pairs are Co ones. Besides, as the Co concentration increases above $x=0.4$, the number of AF pairs of Co spins distant by $2a$ is reduced to the benefit of pairs distant by a or more complex Co clusters.

D. Quasielastic width as a function of temperature

This quasielastic linewidth, half-width at half-maximum (HWHM), is shown in Fig. 11. It does not depend much on x . In a freezing process, the linewidth Γ is equal to the inverse of the relaxation time, so that it is expected to decrease when the spins fluctuations slow down. At the freezing temperature $T_G \sim 50$ K, a minimum of $\Gamma(T)$ is observed. Such minimum has been observed in some spin glasses¹⁹ as well as in Fe-YBCO, either AF or SC, for the Fe spin fluctuations.^{16,20} It could be understood as follows. Below T_G , the slowest spins are frozen and no longer seen in the quasielastic signal; the increase of Γ reveals the existence of fast fluctuations which coexist with the spin freezing, in agreement with the temperature dependence of the elastic and quasielastic intensities. In contrast with Fe-YBCO, the temperature T_G is constant with x , from $x=0.18$ to $x=0.72$, suggesting that the involved spin population is about the same in all samples, whatever they are SC or AF. This can be related to the fact that the freezing spins are mainly $d=2a$ Co-Co pairs even at the highest concentration, $x=0.72$. Assuming as a first approximation, that for $x=0.42$, the quasielastic signal C_2 between 75 and 150 K stems from one kind of spin only (AF Co pairs distant by $d \sim 2a$), one can deduce an activation energy for those pairs through an Arrhenius fit of $\Gamma(T)$ above T_G . One gets $E \sim 10$ meV (inset Fig. 11).

E. Value of the Co magnetic moment

The quasielastic intensity, C_2 , is directly proportional to the paramagnetic susceptibility, $\chi(T)$, according to the relation

TABLE II. Mean values of the Co moments in the oxygenated samples as a function of the Co concentration, deduced from ΔC_2 , ΔC_1 , and susceptibility.

x	SC/AF	1	2	3
		$\mu_{QE}/Co1$ (μ_B) ΔC_2	$\mu_E/Co1$ (μ_B) ΔC_1	$\mu_{para}/Co1$ (μ_B) susceptibility
0.18 ^a	SC	2.6(3)	3.7(4)	3.4(2)
0.42		2.1(2)	3.5(3)	3.2(2)
0.48	AF	2.0(2)		3.4(2)
0.72	AF	1.6(2)	2.6(3)	3.3(2)

^aData taken from Ref. 18.

$$C_2 = \left(\frac{\gamma e^2}{mc^2} \right)^2 F^2(q) \chi(T) \frac{kT}{2\mu_B^2}, \quad (2)$$

where $F(q)$ is the Co magnetic form factor. For N moments equal to μ , $\chi(T)$ is written as $\chi(T) = N\mu^2/3kT$. One can thus deduce the mean value μ_{QE} of the moments that give rise to the quasielastic signal from the signal intensity, C_2 . This intensity was calibrated in absolute scale using a vanadium standard. Table II gives the μ values determined for the different samples of the INS experiment. Column 1 gives the mean value of the magnetic moments that give rise to the quasielastic signal observed at 100 K, column 2 gives the mean value μ_E of the moments that freeze (and appear in the elastic signal) below 150 K. Column 3 gives the value of the mean paramagnetic moment μ_{para} deduced from the susceptibility measurement between 90 and 300 K (see Table I).

The comparison between columns 1 and 3 shows that, as expected, the quasielastic signal attributed mainly to $d \sim 2a$ AF Co-Co pairs, is always smaller than it would be if all Co moments were contributing to it. If we compare columns 2 and 3, we see, that, at low concentrations ($x \leq 0.42$, samples not LR AF ordered at low temperature), about all the paramagnetic moments measured between 300 and 90 K by magnetization (column 3) freeze below 150 K (column 2). This shows that, when the temperature goes down below 150 K, not only the $d \sim 2a$ pairs are slowed down so as to appear in the elastic intensity but also the more rapidly fluctuating uncorrelated moments and $d=a$ pairs.

For $x=0.72$, Table II shows that there are less fluctuating $d \sim 2a$ Co pairs contributing to the quasielastic signal at 100 K (column 1) than for $x \leq 0.42$. Moreover and contrary to the low concentrations, the average static moment $\mu_E/Co1$ measured by ΔC_1 (column 2) is smaller than the paramagnetic moment (column 3). It means that in this AF concentrated sample, part of the moments must become static already above 175 K. This is best shown by adding C_1 and C_2 , which cancels the contribution of the moments transferred from the quasielastic to the elastic signal (diamonds in Fig. 9). As T goes up, we notice that C_1+C_2 seems to flatten for $x=0.42$, whereas it continues decreasing for $x=0.72$. This regular decrease is too large to be attributed to a Debye-Waller effect. It suggests a gradual freezing of fluctuating moments for $x=0.72$, which occurs already above 175 K.

These two behaviors, for $x=0.42$ and $x=0.72$, are, respectively, similar to those observed in SC YBCO-Fe (Refs. 16 and 21) and AF YBCO-Fe (Ref. 20). That a gradual freezing starts to occur at high temperatures (above 150 K) in the $x=0.72$ sample can explain why the magnetization data cannot be fitted by a simple Curie-Weiss law, with C and values independent of T_{\min} in the interval $90 < T_{\min} < 150$ K.

Finally, in this AF sample compared to the dilute samples, there are more frustrated pairs, more complex structures, and the Co moments start to freeze from higher temperatures, a small fraction of them being LR AF ordered already at $T=370$ K.

F. Summary of INS results

The q dependence of the quasielastic intensity measured at 75 K for $x=0.42$ shows that the moments responsible for this signal are fluctuating Co1 pairs distant by $d \sim 2a$. These pairs freeze below 100 K.

The experiment also evinces more rapidly fluctuating spins that are not seen in the quasielastic signal above 100 K but as a “flat” background in the inelastic spectrum. The fluctuations of these spins slow down when T decreases, so that they start contributing to the quasielastic signal below 100 K; they freeze and start contributing to the elastic signal at a still lower temperature. Since at low concentration, they represent more than 50% of the Co moments, they are most likely uncorrelated moments and $d=a$ pairs.

In the $x=0.72$ sample which is LR AF ordered below 370 K, some Co spins are slowed down as compared to the dilute samples, either by their interaction with neighboring spins or by their interaction with the LR ordered moments.

VII. CONCLUSION

The diffraction results are best interpreted by assuming that the Co1 spins are lying preferentially along the c axis while the Cu2 spins are lying preferentially along the a axis. The Co1 moments have a small component, antiparallel to the Cu2 ones, that increases with the Co concentration.

At high Co concentration (or in fully deoxygenated samples), when the LR magnetic order is well established, the mean ordered magnetic moment on the Cu2 sites is close

to that in YBCO6 ($0.63\mu_B$), but the mean ordered magnetic moment on the Cu1 sites, $\mu_0(\text{Cu1}) \leq 0.8\mu_B$, is much lower than the paramagnetic moment determined by magnetization. The INS results give a basis to explain this issue by evidencing different kinds of spins in the fully oxygenated samples: (i) spins that are seen in the quasielastic signal from high temperature to around 50 K where they freeze. These spins are AF Co-Co pairs distant by $d \sim 2a$. They amount to about one-half to one-third of all Co spins in the nonordered samples ($x \leq 0.42$). (ii) More rapidly fluctuating spins, which are present in all Co-YBCO7 samples. They are likely uncorrelated Co spins at low Co concentration samples, together with $d=a$ AF Co pairs at higher concentration. The competition between the two kinds of AF correlations, $d=2a$ and $d=a$ pairs, at high Co concentration, opposes the establishment of a LR AF order for the Co moments. (iii) More complex Co clusters (such as Co pairs interacting with LR ordered moments) in the LR AF ordered $x=0.72$ sample.

If we take into account all these spins (those slowly and those rapidly fluctuating), the mean value of the moment per Co ion given by the INS experiment can be considered to keep a value of $3.5 \pm 0.5\mu_B/\text{Co1}$, constant with the Co concentration.

The Co moments that are LR ordered at low temperature in the AF samples are thus only a small fraction of the whole Co moments since $\mu(\text{Co1})$ remains $\leq 0.8\mu_B$, instead of $3.5\mu_B$, for the following reasons: (i) The Co1-Cu2 interaction is weaker than the Co1-Co1 ones, so that the Cu2 AF LR order is not sufficient to order the Co spins. (ii) The Co1 spins do not order by themselves in the Cu1 planes because of frustration phenomena. Combining the three techniques of neutron diffraction, INS, and magnetization therefore provides a self-consistent picture of the spin correlations and fluctuations in the Co-YBCO series.

ACKNOWLEDGMENTS

The authors thank F. Bourée for the neutron measurements on 3T2 diffractometer, D. Colson for the magnetization measurements, R. Kahn and J. M. Zanotti for their help in the INS measurements on Mibemol spectrometer. The authors also thank P. Bourges for useful discussions and for a critical reading of this paper.

¹F. Bridges, J. B. Boyce, T. Claeson, T. H. Geballe, and J. M. Tarascon, Phys. Rev. B **39**, 11603 (1989).

²R. S. Howland, T. H. Geballe, S. S. Laderman, A. Fischer-Colbrie, M. Scott, J. M. Tarascon, and P. Barboux, Phys. Rev. B **39**, 9017 (1989).

³H. Renevier, J. L. Hodeau, M. Marezio, and A. Santoro, Physica C **220**, 143 (1994).

⁴P. F. Miceli, J. M. Tarascon, L. H. Greene, P. Barboux, F. J. Rotella, and J. D. Jorgensen, Phys. Rev. B **37**, 5932 (1988).

⁵J. F. Bringley, T.-M. Chen, B. A. Averill, K. M. Wong, and S. J. Poon, Phys. Rev. B **38**, 2432 (1988).

⁶M. Kakihana, L. Börjesson, S. Eriksson, P. Svedlindh, and P.

Norling, Phys. Rev. B **40**, 6787 (1989).

⁷P. F. Miceli, J. M. Tarascon, L. H. Greene, P. Barboux, M. Giroud, D. A. Neumann, J. J. Rhyne, L. F. Schneemeyer, and J. V. Waszczak, Phys. Rev. B **38**, 9209 (1988).

⁸P. Zolliker, D. E. Cox, J. M. Tranquada, and G. Shirane, Phys. Rev. B **38**, 6575 (1988).

⁹F. Maury, I. Mirebeau, J. Hodges, P. Bourges, Y. Sidis, and A. Forget, Phys. Rev. B **69**, 094506 (2004).

¹⁰J. Rodríguez-Carvajal, Physica B **192**, 55 (1993); FULLPROF, URL <ftp://ftp.cea.fr/pub/lhb/divers/Fullprof>

¹¹J. Rossat-Mignod, P. Burlet, M. J. Jugens, C. Vettier, L. P. Regnault, J. Y. Henry, C. Ayache, L. Forro, H. Noel, M. Potel, P.

- Gougeon, and J. C. Levet, *J. Phys. (France)* **49**, C8-2119 (1988).
- ¹²S. Shamoto, M. Sato, J. M. Tranquada, B. J. Sternlieb, and G. Shirane, *Phys. Rev. B* **48**, 13817 (1993).
- ¹³H. Casalta, P. Schleger, E. Brecht, W. Montfrooij, N. H. Andersen, B. Lebech, W. W. Schmahl, H. Fuess, Ruixing Liang, W. N. Hardy, and T. Wolf, *Phys. Rev. B* **50**, 9688 (1994).
- ¹⁴P. Burllet, J. Y. Henry, and L. P. Regnault, *Physica C* **296**, 205 (1998).
- ¹⁵I. Mirebeau, M. Hennion, G. Coddens, T. E. Phillips, and K. Moorjani, *Europhys. Lett.* **9**, 181 (1989).
- ¹⁶M. Hennion, I. Mirebeau, G. Coddens, A. Menelle, T. E. Phillips, K. Moorjani, and M. Hervieu, *Physica C* **159**, 124 (1989).
- ¹⁷For a review see Y. Sidis, S. Pailh s, B. Keimer, P. Bourges, C. Ulrich, and L. P. Regnault, *Phys. Status Solidi B* **241**, 1204 (2004).
- ¹⁸C. Bellouard, M. Hennion, I. Mirebeau, A. J. Dianoux, and V. Caignaert, *J. Magn. Magn. Mater.* **104-107**, 517 (1992).
- ¹⁹C. Bellouard, M. Hennion, I. Mirebeau and B. Hennion, *J. Magn. Magn. Mater.* **104-107**, 1627 (1992).
- ²⁰I. Mirebeau, C. Bellouard, M. Hennion, G. Jehanno, V. Caignaert, A. J. Dianoux, T. E. Phillips, and K. Moorjani, *Physica C* **184**, 299 (1991).
- ²¹M. Hennion, I. Mirebeau, L. Boudarene, C. Bellouard, G. Jehanno, A. J. Dianoux, and V. Caignaert, *Physica B* **180-181**, 440 (1992).